Overview of Performance Lower Bounds for Blind Frequency-Offset Estimation

Nele Noels
Philippe Ciblat
Heidi Steendam

Abstract

This paper focuses on performance bounds for estimating the frequency and the phase of a received signal when the complex amplitude of the signal is non-constant and unknown. Receivers need to perform such an estimation in many application fields, including digital communications, direction-of-arrival estimation, and Doppler radar. While in digital communications the non-constant complex-signal amplitude is a discrete random variable related to the transmitted information bits, in many other signal-processing fields this non-constant amplitude is typically modeled as multiplicative Gaussian noise. Fundamental lower bounds on the mean square error of any frequency-offset and phase-shift estimator are continuously employed in all these application fields. They serve as a useful benchmark for judging the performance of practical estimators. We present an overview of such bounds with their respective areas of interest, and their associated derivations in closed form.

1. Introduction and Motivation

Let us consider digital bandpass communication over an additive white Gaussian noise (AWGN) channel, using linear modulation. An information bit sequence is first channel-encoded, and then mapped to a block of complex numbers (data symbols) belonging to a discrete symbol constellation set, Ω. The *channel encoder* introduces structured redundancy in the transmitted bit sequences: this makes it possible to detect and correct at the receiver some of the bit errors that have occurred. *Symbol mapping* is performed to improve the bandwidth efficiency. The resulting data symbols are first applied to a square-root Nyquist transmitting filter, and then multiplied to a sinusoidal transmitting carrier signal in order to obtain a signal that is suitable for transmission over the bandpass channel. At the receiver end, the received signal is multiplied with a carrier signal matched to the transmitted carrier signal, applied to a filter matched to the transmitting filter, and sampled at the correct instants in time.

To enable reliable detection of the transmitted information bits from the resulting observation samples, it is imperative that the carrier signals at the transmitter and the receiver have almost exactly the same frequency and phase. However, as the carrier oscillators at the transmitter and receiver operate independently, their frequency and phase are not the same. The demodulation at the receiver is performed using a local reference carrier signal that exhibits a frequency offset, φ_1, and a phase shift, $2\pi\varphi_0$, vis-à-vis the received modulated carrier signal. In this case, the observation samples can be modeled as a noisy version of a complex sinusoid with frequency φ_1 and phase $2\pi\varphi_0$ and with a non-constant complex-valued amplitude equal to the unknown transmitted data symbols or realizations of a multiplicative Gaussian noise process. In order to cope with the unknown parameters, φ_0 and φ_1, the receiver is fitted with an estimation unit, which has to estimate the quantities φ_0 and φ_1 from the observation samples. Once the frequency offset and the phase shift have been estimated, the demodulated signal is *corrected* in order to compensate for them. The detection unit of the receiver subsequently decides upon the received information bits based on the corrected observation samples, assuming perfect frequency-offset and phase-shift compensation. A result of the latter assumption is that the accuracy of the estimation unit has direct repercussions on the accuracy of the detection unit.

Aside from a mismatch between the transmitting and receiving carrier frequency, the frequency offset, φ_1, can also result from the Doppler effect. If a vehicle is transmitting information to the receiver side and is simultaneously moving, the transmitted carrier frequency is modified by

Nele Noels and Heidi Steendam are with the Department of Telecommunications and Information Processing, University of Gent, St-Pietersnieuwstraat 41, B-9000 Gent, Belgium; E-mail: nele.noels@telin.ugent.be. Philippe Ciblat is with TELECOM ParisTech (formerly, Ecole Nationale Supérieure des Télécommunications), Communications and Electronics Department, Digital Communications Research Team, 46 rue Barrault, 75013 Paris; E-mail: PhilippeCiblat@telecom-paristech.fr.

This is an invited *Review of Radio Science* from Commission C.

the Doppler effect, and the receiver is not well adapted in frequency. This Doppler effect – which is a drawback in digital communications – can be of great interest in some applications. For instance, radar based on the Doppler effect is able to find the velocity of a target. In other applications, such as direction-of-arrival (DOA) estimation, the spatial frequency related to the angle-of-arrival in an array processing can be mathematically seen as a carrier-frequency offset. As a consequence, besides digital communications, there are a lot of applications for which estimating a frequency disturbed by a non-constant amplitude is needed. Unlike digital communications, this non-constant amplitude is not associated with information bits, but with other parameters, such as the Doppler spread for Doppler radar, or the spatial distribution of the source for direction-of-arrival estimation [1-3].

The estimation accuracy is usually measured by the mean square estimation error (MSEE). This is the expected value of the squared difference between the estimated and the true values of the frequency offset and the phase shift. The estimation unit that minimizes the mean square estimation error is referred to as the *minimum mean square error* (MMSE) estimator. In many practical situations, minimum mean square error estimation gives rise to a prohibitive computational burden, and one has to resort to approximation techniques. The various existing estimation units are the result of applying these techniques (see, e.g., [4]).

Rapid developments in digital communications [5-8] and signal-processing applications [1-3] have caused a nonstop increase in the requirements that are imposed on the estimation units' design. This has also provided a constant impulse to the research on the fundamental lower bounds on the attainable estimation accuracy (see, e.g., [1-3, 9-20, 20-31]). On the one hand, such bounds serve as a useful benchmark for judging the performance of practical estimators. On the other hand, if interpretable closed-form expressions exist, they also might provide useful insight into the influence of the various signal parameters on the achievable estimation accuracy.

In this tutorial, we focus on the derivation and the analysis of such bounds. One of the most celebrated performance limits is the Cramer-Rao bound (CRB) [32], which is known to be a tight bound for a wide class of estimators, provided that the SNR (signal-to-noise ratio) is sufficiently high. In the applications considered, the statistics of the observation samples depend not only on the frequency offset and the phase shift to be estimated, but also on the statistics of the non-constant amplitude. This makes the computation of the Cramer-Rao bound far from trivial. In order to avoid the computational complexity associated with the true Cramer-Rao bound, several alternative Cramer-Rao-like bounds have also been proposed in the literature (see, e.g., [2, 9, 10, 14, 26, 31]). We present an overview of these bounds with their respective areas of interest and their associated derivations in closed-form for various cases (coded/non-coded digital modulation, circular/non-circular multiplicative noise). It is well known that the Cramer-Rao bound (and, in particular, the Cramer-Rao bound for frequency-offset estimation) is not accurate at low SNR and/or when the number of observation samples becomes too small [33]. The large gap between the Cramer-Rao bound and the mean- square estimation error of practical frequency-offset estimators is the result of the estimators sporadically making large errors, referred to as outliers. To analyze this phenomenon, we also discuss the Barankin bound (BB) [27-29] and the Ziv-Zakai bound (ZZB) [20] for frequency-offset estimation. These are more-complicated bounds to compute, but they are considerably tighter than the Cramer-Rao bound at low SNR.

2. Problem Formulation

Throughout the paper, the following signal model is considered:

$$r(n) = a(n)e^{2\pi j(\varphi_0 + \varphi_1 n)} + w(n), \qquad (1)$$

for $n = k_0, ..., k_0 + N - 1$, where:

- $a(n)$ is a priori unknown and is referred to as either "multiplicative noise" or "non-constant amplitude."
- φ_0 and φ_1 are the normalized phase shift (at $n = 0$) and the normalized frequency offset of the received signal, respectively. These parameters are also a priori unknown to the receiver and need to be estimated. The absolute value of k_0 determines the difference (in number of symbol intervals) between the start of the received signal and the time instant at which the phase shift, φ_0, is estimated.
- $w(n)$ is circularly symmetric complex-valued additive white Gaussian noise with zero mean, and variance σ_w^2.

By stacking all the available observations into a row vector, we have

$$\mathbf{r} = \mathbf{a}\mathbf{S}\left([\varphi_0, \varphi_1]\right) + \mathbf{w}, \qquad (2)$$

where:

- $\mathbf{w}$ is a Gaussian noise vector with zero mean, $\mathbb{E}\left[\mathbf{w}^{\mathrm{T}}\mathbf{w}\right] = \mathbf{0}_N$, and $\mathbb{E}\left[\mathbf{w}^{\mathrm{H}}\mathbf{w}\right] = \sigma_w^2\mathbf{I}_N$, where $\mathbf{0}_k$ represents a $k \times k$ null matrix, and $\mathbf{I}_k$ represents a $k \times k$ identity matrix. The superscripts $(\cdot)^{\mathrm{T}}$ and $(\cdot)^{\mathrm{H}}$ stand for the transposition and the conjugate-transposition operators, respectively.

- $\mathbf{S}\left([\varphi_0,\varphi_1]\right)$ is a diagonal matrix with the *n*th diagonal element given by

$$S\left(n,n;[\varphi_0,\varphi_1]\right)=e^{2\pi j(\varphi_0+\varphi_1 n)},$$

such that

$$\mathbf{S}\left([\varphi_0,\varphi_1]\right)\mathbf{S}^{\mathrm{H}}\left([\varphi_0,\varphi_1]\right)=\mathbf{I}_N.$$

The signal model of Equations (1) and (2) is encountered in several application fields. A first example is that of digital bandpass communication over an additive-white-Gaussian-noise channel using linear modulation. In that case, $a(n)$ represents the *n*th data symbol passing through the digital bandpass communication channel. The data symbols result from an information bit sequence that is first channel encoded (for better bit-error protection), and then mapped (for higher-bandwidth utilization) to a block of complex numbers belonging to a discrete set Ω, referred to as the symbol constellation. In the digital-communications case, we will also consider that $\sigma_w^2=N_0/E_s$, with N_0 and E_s assumed to be known. Here, N_0 denotes the noise-power spectral density, and E_s is the symbol energy. The ratio E_s/N_0 is an important measure of the signal quality at the receiver, and is commonly referred to as the *signal-to-noise ratio* (SNR).

As already stated, other application fields where the signal model of Equation (1) can be encountered are that of direction-of-arrival estimation and Doppler radar. In direction-of-arrival estimation, $a(n)$ represents the spatial distribution of the source. In Doppler radar, $a(n)$ represents the Doppler spread of the reference signal. In both cases, it is standard to model the non-constant amplitude as a Gaussian process [1, 3, 34]. Even in digital communications, the process $a(n)$ can sometimes be viewed as a Gaussian process: indeed, in a flat fading channel, $a(n)$ can be the product between a transmitted symbol and a non-constant complex amplitude related to the channel quality. Due to the various scatterers, in a non-line-of-sight (NLOS) channel it is usual to consider that non-constant amplitude as a Gaussian process, and there for to consider its magnitude as a Rayleigh process. It is therefore also referred to as the Rayleigh channel (e.g., [35]).

For the sake of completeness, we note that Equation (1) is only approximate and, in particular, valid only when $|\varphi_1|\ll 1$ [15].

From the observation samples $\{r(n)\}$ in Equation (1), we now want to recover the value of a deterministic parameter vector $\mathbf{u}$ with components u_0, u_1, ... This vector contains (but is not restricted to) the unknown phase shift, φ_0, and the frequency offset, φ_1. A common approach to evaluate the quality of an unbiased estimator for $\mathbf{u}$ consists in comparing its resulting mean-square estimation error with a Cramer-Rao bound, or some other tight, fundamental lower bound on the achievable mean-square estimation error.

3. Deriving the Cramer-Rao Bound

The Cramer-Rao bound results from the inequality $\mathbf{R_u}-\mathbf{J}^{-1}\geq\mathbf{0}$ [32]. Here, $\mathbf{R_u}$ is the error correlation matrix related to the estimation of a deterministic parameter vector $\mathbf{u}$. The notation $\mathbf{A}\geq\mathbf{0}$ indicates that $\mathbf{A}$ is a positive semi-definite matrix, and $\mathbf{J}^{-1}$ denotes the inverse of the Fisher information matrix (FIM), $\mathbf{J}$. The elements of $\mathbf{J}$ are given by

$$J_{u_k,u_l}=\mathbb{E}\left[\ell_k(\mathbf{u};\mathbf{r})\,\ell_l(\mathbf{u};\mathbf{r})\right], \qquad (3)$$

where J_{u_k,u_l} corresponds to the joint Fisher information for the parameters (u_k,u_l), where $\mathbb{E}[\cdot]$ denotes averaging with respect to $p(\mathbf{r}\,|\,\mathbf{u})$, and where

$$\ell_k(\mathbf{u};\mathbf{r})=\frac{\partial \ln p(\mathbf{r}|\mathbf{u})}{\partial u_k}$$

is a shorthand notation for the derivative of $\ln p(\mathbf{r}|\mathbf{u})$ with respect to the *k*th parameter, u_k, of $\mathbf{u}$. It easily follows from $\mathbf{R_u}-\mathbf{J}^{-1}\geq\mathbf{0}$ that

$$\mathbb{E}\left[(u_k-\hat{u}_k)^2\right]\geq \mathrm{CRB}(u_k), \qquad (4)$$

where $\mathrm{CRB}(u_k)$ is the *k*th diagonal element of the inverse of the Fisher information matrix, **J**. The right-hand side of the above expression is referred to as the Cramer-Rao bound.

3.1 Non-Constant Complex Amplitude = Digital Data Symbol

In this section we derive the exact Cramer-Rao bound – or, equivalently, the exact Fisher information matrix – for the deterministic parameter vector $\mathbf{u}=[u_0,u_1]=[\varphi_0,\varphi_1]$ from *N* samples of a received linearly modulated digital communication signal in additive white Gaussian noise. We recall that we consider the signal model given by Equations (1) and (2). As is usually done in digital communications, we model the symbol vector, **a,** as a discrete random vector with the following uniform a priori distribution:

$$\Pr\left[\mathbf{a}=\tilde{\mathbf{a}}\right]=\begin{cases}2^{-N_b}, & \tilde{\mathbf{a}}\in\mathcal{S}_0\\ 0, & \tilde{\mathbf{a}}\in\mathcal{S}\setminus\mathcal{S}_0\end{cases}. \qquad (5)$$

Here, $\mathcal{S}$ denotes the set of all possible vectors of N symbols taking values in the symbol constellation set Ω, and $\mathcal{S}_0\subset\mathcal{S}$ denotes the subset of these vectors that result from encoding and mapping an information bit sequence. The distribution of Equation (5) reflects that a one-to-one correspondence exists between the set of all possible sequences of N_b information bits and the data symbol vectors in S_0, while the receiver has no prior knowledge about the transmitted information bit sequence. It is further standard to assume that $\mathbb{E}\left[\mathbf{a}\right]=0$ and that $\mathbb{E}\left[\mathbf{a}^{\mathrm{H}}\mathbf{a}\right]=\mathbf{I}_N$. This assumption holds true for transmissions without channel encoding, and is approximately valid for most practical coded-modulation schemes [36].

A brute-force numerical evaluation of the Fisher information matrix related to the estimation of $\mathbf{u}$ involves replacing the statistical average $\mathbb{E}[\cdot]$ in Equation (3) by an arithmetical average over a large number of realizations of $\mathbf{r}$ that are computer-generated according to the conditional distribution $p\left(\mathbf{r}\,|\,\mathbf{u}\right)$. The numerical evaluation of the Fisher information matrix further requires the computation of the derivatives $\ell_k\left(\mathbf{u};\mathbf{r}\right)$, $k=0,1$, which correspond to the realizations of $\mathbf{r}$ given $\mathbf{u}$. These derivatives can be put into the following form [37]:

$$\ell_k\left(\mathbf{u};\mathbf{r}\right)=\sum_{\tilde{\mathbf{a}}}\frac{\partial\ln p\left(\mathbf{r}\left|\mathbf{a}=\tilde{\mathbf{a}},\mathbf{u}\right.\right)}{\partial u_k}\Pr\left[\mathbf{a}=\tilde{\mathbf{a}}\left|\mathbf{r},\mathbf{u}\right.\right]. \qquad (6)$$

As $\mathbf{p}\left(\mathbf{r}\left|\mathbf{a},\mathbf{u}\right.\right)$ is Gaussian, the logarithm $\ln p\left(\mathbf{r}\left|\mathbf{a},\mathbf{u}\right.\right)$ is readily available in closed form:

$$\ln p\left(\mathbf{r}\left|\mathbf{a},\mathbf{u}\right.\right)\propto-\frac{E_s}{N_0}\left|\mathbf{r}-\mathbf{a}\mathbf{S}\left(\mathbf{u}\right)\right|^2.$$

Differentiating with respect to u_k yields

$$\frac{\partial\ln p\left(\mathbf{r}\left|\mathbf{a},\mathbf{u}\right.\right)}{\partial u_k}=-\frac{2E_s}{N_0}\Re\left\{\left[\mathbf{r}-\mathbf{a}\mathbf{S}\left(\mathbf{u}\right)\right]^{\mathrm{H}}\left[\mathbf{a}\frac{\partial\mathbf{S}\left(\mathbf{u}\right)}{\partial u_k}\right]\right\}$$

The joint symbol a posteriori probabilities (APP) $\Pr\left[\mathbf{a}\left|\mathbf{r},\mathbf{u}\right.\right]$ in Equation (6) can be computed from $p\left(\mathbf{r}\left|\mathbf{a},\mathbf{u}\right.\right)$ and $\Pr\left[\mathbf{a}\right]$ according to

$$\Pr\left[\mathbf{a}\left|\mathbf{r},\mathbf{u}\right.\right]=\frac{\Pr\left[\mathbf{a}\right]p\left(\mathbf{r}\left|\mathbf{a},\mathbf{u}\right.\right)}{\sum_{\tilde{\mathbf{a}}}p\left(\mathbf{r}\left|\mathbf{a}=\tilde{\mathbf{a}},\mathbf{u}\right.\right)\Pr\left[\mathbf{a}=\tilde{\mathbf{a}}\right]}. \qquad (7)$$

Although this procedure yields the exact derivatives $\ell_k\left(\mathbf{u};\mathbf{r}\right)$, $k=0,1$, the summations in Equations (6) and (7) give rise to a computational complexity that is exponential in the burst size, N.

It was shown in [16] and [37] that the computational complexity associated with the evaluation of the Cramer-Rao bound can be drastically reduced by taking into account the specific (linearly modulated) structure of the useful signal in Equation (1).

Because $\mathbf{S}\left(\mathbf{u}\right)\mathbf{S}^{\mathrm{H}}\left(\mathbf{u}\right)=\mathbf{I}_N$ does not depend on $\mathbf{u}$, we obtain

$$\frac{\partial\ln p\left(\mathbf{r}\left|\mathbf{a},\mathbf{u}\right.\right)}{\partial u_k}=\frac{2E_s}{N_0}\Re\left\{\mathbf{r}\left[\frac{\partial\mathbf{S}\left(\mathbf{u}\right)}{\partial u_k}\right]^{\mathrm{H}}\mathbf{a}^{\mathrm{H}}\right\}.$$

Substituting the above expression into Equation (6) then yields

$$\ell_k\left(\mathbf{u};\mathbf{r}\right)=\frac{2E_s}{N_0}\Re\left\{\mathbf{r}\left(\frac{\partial\mathbf{S}\left(\mathbf{u}\right)}{\partial u_k}\right)^{\mathrm{H}}\boldsymbol{\mu}^{\mathrm{H}}\left(\mathbf{r},\mathbf{u}\right)\right\}, \qquad (8)$$

where $\boldsymbol{\mu}\left(\mathbf{r},\mathbf{u}\right)$ is a shorthand notation for the a posteriori average of the symbol vector $\mathbf{a}$ with N components:

$$\mu\left(n;\mathbf{r},\mathbf{u}\right)=\mathbb{E}_{\mathbf{a}}\left[a\left(n\right)\left|\mathbf{r},\mathbf{u}\right.\right] \qquad (9)$$

$$=\sum_{\omega\in\Omega}\omega\Pr\left[a\left(n\right)=\omega\left|\mathbf{r},\mathbf{u}\right.\right], \qquad (10)$$

where Ω denotes the set of constellation points, and the averaging $\mathbb{E}_{\mathbf{a}}\left[\cdot\left|\mathbf{r},\mathbf{u}\right.\right]$ is with respect to $\Pr\left[\mathbf{a}\left|\mathbf{r},\mathbf{u}\right.\right]$. We emphasize that no approximation is involved in obtaining Equation (10): the right-hand side simply expresses the a posteriori average of the nth data symbol $a\left(n\right)$ in terms of the *marginal* a posteriori probabilities of $a\left(n\right)$, rather than the *joint* a posteriori probabilities of all components of $\mathbf{a}$.

Computing the marginal a posteriori probabilities from the joint a posteriori probabilities still requires a complexity that increases exponentially with N. However, in most practical scenarios, the required marginal symbol a posteriori probabilities can be directly computed in an efficient way by applying the sum-product algorithm to a factor graph (FG) representing a suitable factorization of the joint-symbol a posteriori probabilities [38]. The application of the sum-product algorithm on a graph that

corresponds to a tree (i.e., a cycle-free factor graph) is straightforward, and yields the exact marginals. When the graph contains cycles, the sum-product algorithm becomes an iterative procedure that yields only an approximation of the marginals after convergence. However, when the cycles in the graph are large, the resulting marginals turn out to be quite accurate. When using this factor-graph-based approximation technique to compute the required marginal symbol a posteriori probabilities, computing the derivatives $\ell_k(\mathbf{u};\mathbf{r})$, $k=0,1$ according to Equation (8) for a given realization of **r** given **u** yields a complexity that is linear (and not exponential) in the number of data symbols *N*. The above expression and evaluation procedure is the main result for the Cramer-Rao bound derivations. It allows a fast evaluation of the Cramer-Rao bound, and holds for any channel code and any symbol constellation.

For specific hypotheses about the channel code and the symbol constellation, the complexity associated with evaluating the Fisher information matrix, or, equivalently, the Cramer-Rao bounds, can be further reduced (see, e.g., [12-13, 15, 19]). We mention a result from [15] for arbitrarily mapped uncoded linear modulation. In that case, all transmitted data symbols are statistically independent and equi-probable, such that the a priori distribution of **a**, Equation (5), reduces to

$$\Pr[\mathbf{a}=\tilde{\mathbf{a}}]=2^{-N_b},\ \forall\tilde{\mathbf{a}}\in\mathcal{S}. \tag{11}$$

Taking into account Equation (11), it is easily verified from Equations (9), (10), and (7) that the components of the a posteriori average of the data-symbol vector **a** reduce to

$$\mu[n;r(n),\mathbf{u}]=\frac{\sum_{\omega\in\Omega}\omega e^{\left\{\frac{E_s}{N_0}\left[2\Re\left\{r(n)e^{-2\pi j(\varphi_0+\varphi_1 n)}\omega^*\right\}-|\omega|^2\right]\right\}}}{\sum_{\omega\in\Omega}e^{\left\{\frac{E_s}{N_0}\left[2\Re\left\{r(n)e^{-2\pi j(\varphi_0+\varphi_1 n)}\omega^*\right\}-|\omega|^2\right]\right\}}}, \tag{12}$$

which only depend on **r** through $r(n)$. Taking this into account, it was shown in [15] that with *N* odd-valued and $k_0=-\frac{1}{2}(N-1)$ (i.e., φ_0 is the phase shift at the burst center), the Cramer-Rao bounds can be written in the following form:

$$\left[\mathrm{CRB}(\varphi_0)\right]^{-1}=8\pi^2\frac{E_s}{N_0}NR_\Omega\left(\frac{E_s}{N_0}\right), \tag{13}$$

$$\left[\mathrm{CRB}(\varphi_1)\right]^{-1}=\left[\mathrm{CRB}(\varphi_0)\right]^{-1}\frac{\left(N^2-1\right)}{12}, \tag{14}$$

where

$$R_\Omega\left(\frac{E_s}{N_0}\right)=\frac{2E_s}{N_0}\mathbb{E}\left[\Im\left\{\mu^*[n;r(n),\mathbf{u}]r(n)S^*(n,n;\mathbf{u})\right\}^2\right] \tag{15}$$

It was further shown in [15] that $J_{\varphi_0,\varphi_1}=J_{\varphi_1,\varphi_0}=0$. This means that the estimation of the phase shift, φ_0, at the center of the observation interval is independent of the frequency (φ_1) estimation problem. We observe that $\mathrm{CRB}(\varphi_0)$ is inversely proportional to the number of available signal samples, *N*, whereas $\mathrm{CRB}(\varphi_0)$ is inversely proportional to $N\left(N^2-1\right)\approx N^3$, where the approximation holds for large *N*. We further observe that $\mathrm{CRB}(\varphi_0)$ and $\mathrm{CRB}(\varphi_1)$ are proportional to the same factor $R_\Omega\left[\frac{E_s}{N_0}\right]$ that depends on the symbol constellation and on the SNR, but not on the number of available signal samples. The numerical evaluation of the Cramer-Rao bounds from Equations (13) and (14) involves replacing the statistical average $\mathbb{E}[\cdot]$ in Equation (15) by an arithmetical average over a large number of realizations of $r(n)S^*(n,n;\mathbf{u})$. This procedure is significantly less complex than the evaluation of the Fisher information matrix entries according to Equations (3) and (8)-(10) using the factor-graph-approach, because the a posteriori symbol average, Equation (12), is available in closed form, and the average that needs to be computed in Equation (15) is with respect to a complex-valued *scalar*, rather than a complex-valued vector of size *N*.

In spite of all the efforts made in the literature with respect to computing the Fisher information matrix for linear modulation, an explicit analytical closed-form expression for the Cramer-Rao bounds still does not exist. The main contributions of the research conducted in [12-13] and [15-19] was in the derivation of new procedures that allow a more-efficient (hence, faster) numerical evaluation of the Cramer-Rao bounds. Unfortunately, the expressions that lead to (and/or come as by-products of) these evaluation procedures usually don't bring much insight into the behavior of the Fisher information matrix (e.g., as a function of the parameters that describe the coded modulation scheme).

We will see in the simulation section of the paper that

- For a given symbol constellation set, Cramer-Rao bounds for coded and uncoded transmission are equal at sufficiently high SNR. However, at lower SNR the Cramer-Rao bound for coded transmission is significantly lower than the Cramer-Rao bound for uncoded transmission.
- For a given channel code, the Cramer-Rao bounds increase when the minimum Euclidean distance between the constellation points decreases.

To avoid the computational complexity associated with the evaluation of the true Cramer-Rao bounds,

asymptotic Cramer-Rao bounds (ACRBs) were considered in [14] and [11] for the case of uncoded linear modulation. This resulted in closed-form analytical expressions for the Cramer-Rao bound that only hold for sufficiently low or high SNR. The high-SNR asymptotic Cramer-Rao bounds are shown to coincide with the modified Cramer-Rao bound (MCRB). This is another lower bound on the mean square estimation error of any unbiased estimator, which is simpler to evaluate but looser than the exact (true) Cramer-Rao bound. We will come back to the modified Cramer-Rao bound later in this paper. For the low-SNR asymptotic Cramer-Rao bounds, the following expressions were presented in [14], assuming N odd valued and $k_0 = -\frac{1}{2}(N-1)$

$$\left[\mathrm{ACRB}(\varphi_0)\right]^{-1}_{|\mathrm{lowSNR}} = 8\pi^2 \left(\frac{E_s}{N_0}\right)^L N \frac{L^2 |f_L|^2}{L!},$$

$$\left[\mathrm{ACRB}(\varphi_1)\right]^{-1}_{|\mathrm{lowSNR}} = \left[\mathrm{ACRB}(\varphi_0)\right]^{-1}_{|\mathrm{lowSNR}} \frac{\left(N^2-1\right)}{12}, \quad (16)$$

where L is related to the symmetry angle $\frac{2\pi}{L}$ of the constellation, and $f_L = \mathbb{E}\left\{\left[a(k)\right]^L\right\}$. We observe that at sufficiently low SNR, the Cramer-Rao bounds are determined by the symmetry angle of the constellation, and evolve in inverse proportion to the Lth power of the SNR.

3.2 Non-Constant Complex Amplitude = A Gaussian Process

We recall that we consider the signal model given by Equation (1). In the rest of this section, we just assume that $k_0 = 0$. However, in this section we add extra assumptions on the non-constant amplitude $a(n)$. As usually done in Doppler radar, direction-of-arrival estimation, or digital communication over a Rayleigh flat-fading channel, the non-constant amplitude, $a(n)$, is assumed to be a zero-mean Gaussian stationary process with correlation $c_a(\tau) = \mathbb{E}\left[a(n+\tau)a^*(n)\right]$ and pseudo-correlation $p_a(\tau) = \mathbb{E}\left[a(n+\tau)a(n)\right]$. The spectrum and pseudo-spectrum are respectively denoted as follows:

$$C_a\left(e^{2i\pi f}\right) = \sum_{\tau\in\mathbb{Z}} c_a(\tau) e^{-2i\pi f\tau}$$

and

$$P_a\left(e^{2i\pi f}\right) = \sum_{\tau\in\mathbb{Z}} p_a(\tau) e^{-2i\pi f\tau}.$$

By construction, one can remark that $P_a\left(e^{2i\pi f}\right) = P_a\left(e^{-2i\pi f}\right)$ Moreover, the entire statistics $\{c_a(\tau), p_a(\tau)\}_{\tau\in\mathbb{Z}}$ of $a(n)$ only depend on a finite number, K, of real-valued unknown parameters, denoted by $\{\alpha_k\}_{k=1,\ldots,K}$. The non-constant amplitude process, $a(n)$, can be real-valued or complex-valued. In the case of a complex-valued process, $a(n)$ can further be *circular* (which means the process distribution is insensitive to any rotation, and thus means that $\mathbb{E}\left[a(n)a(n+\tau)\right] = 0$ for all τ) or *noncircular* (there exists at least one τ_0 such that $\mathbb{E}\left[a(n)a(n+\tau_0)\right] \neq 0$). One can notice that a real-valued process is by definition noncircular. Based on the Cramer-Rao bound, we will see hereafter that the estimation quality can be split into two classes in regard to the circularity/non-circularity property of the process. In contrast, the estimation performance is independent of the nature of the process' values (real or complex). For further information on the non-circularity property, the reader may refer to [15, 39].

Below, we will first derive the Fisher information matrix when the number of available samples, N, is finite (i.e., the non-asymptotic case). Since once again the expression obtained for the Fisher information matrix does not provide additional insights, it is of great interest to further simplify the Fisher information matrix expression by also considering the case for N going to infinity (i.e., the asymptotic case). The resulting Cramer-Rao bounds are referred to as Gaussian Cramer-Rao bounds (GCRB).

3.2.1 Non-Asymptotic Case

We next derive the exact Gaussian Cramer-Rao bound, or, equivalently, the exact Gaussian Fisher information matrix, $\mathbf{J}$, for the deterministic parameter vector $\mathbf{u} = \left[\varphi_0, \varphi_1, \sigma_w^2, \alpha_1, \ldots, \alpha_K\right]$, when N samples of $r(n)$ are available. In order to use well-known results on the Fisher information matrix [40], we work with real-valued processes. We consider $\breve{\mathbf{r}} = \left\{\Re[\mathbf{r}], \Im[\mathbf{r}]\right\}$, which is a multivariate Gaussian variable with zero mean and covariance matrix $\breve{\mathbf{C}}_{\mathbf{r}}$.

The Fisher information matrix for a multivariate Gaussian observation vector $\breve{\mathbf{r}}$ has a special form. As one can check that $\breve{\mathbf{C}}_{\mathbf{r}}$ is symmetric, formula (5.2.1) in [40] holds, and this leads to

$$J_{u_k,u_l} = \frac{1}{2}\mathrm{Tr}\left(\frac{\partial \breve{\mathbf{C}}_{\mathbf{r}}}{\partial u_k}\breve{\mathbf{C}}_{\mathbf{r}}^{-1}\frac{\partial \breve{\mathbf{C}}_{\mathbf{r}}}{\partial u_l}\breve{\mathbf{C}}_{\mathbf{r}}^{-1}\right),$$

where $\mathrm{Tr}(\cdot)$ is the trace operator.

After straightforward algebraic manipulations, we can show that

$$J_{u_k,u_l} = \frac{1}{2}\mathrm{Tr}\left(\frac{\partial \tilde{\mathbf{C}}_{\mathbf{r}}}{\partial u_k}\tilde{\mathbf{C}}_{\mathbf{r}}^{-1}\frac{\partial \tilde{\mathbf{C}}_{\mathbf{r}}}{\partial u_l}\tilde{\mathbf{C}}_{\mathbf{r}}^{-1}\right),$$

where $\tilde{\mathbf{C}}_{\mathbf{r}}$ is the covariance matrix of the random vector $\tilde{\mathbf{r}} = \left[\mathbf{r}, \mathbf{r}^*\right]$, and takes the following form:

$$\tilde{\mathbf{C}}_{\mathbf{r}} = \begin{bmatrix} \mathbf{C}_{\mathbf{r}} & \mathbf{P}_{\mathbf{r}} \\ \mathbf{P}_{\mathbf{r}}^* & \mathbf{C}_{\mathbf{r}}^* \end{bmatrix}$$

with $\mathbf{C}_{\mathbf{r}} = \mathbf{E}\left[\mathbf{r}^{\mathrm{H}}\mathbf{r}\right]$ and $\mathbf{P}_{\mathbf{r}} = \mathbf{E}\left[\mathbf{r}^{\mathrm{T}}\mathbf{r}\right]$.

One can remark that $\tilde{\mathbf{C}}_{\mathbf{r}} = \tilde{\mathbf{S}}\left(\tilde{\mathbf{C}}_{\mathbf{a}} + \sigma_w^2\mathbf{I}_{2N}\right)\tilde{\mathbf{S}}^{\mathrm{H}}$, where $\tilde{\mathbf{S}} = \left\{\mathbf{S}\left[(\varphi_0, \varphi_1)\right], \mathbf{0}_N; \mathbf{0}_N, \mathbf{S}^*\left[(\varphi_0, \varphi_1)\right]\right\}$, and where $\tilde{\mathbf{C}}_{\mathbf{a}}$ is defined in a similar way as $\tilde{\mathbf{C}}_{\mathbf{r}}$. As $\tilde{\mathbf{C}}_{\mathbf{a}}$ does not depend on the phase parameters, we obtain the following expressions for the Fisher information matrix:

$$J_{\alpha_k,\alpha_l}$$

$$= \frac{1}{2}\mathrm{Tr}\left[\frac{\partial\tilde{\mathbf{C}}_{\mathbf{a}}}{\partial\alpha_k}\left(\tilde{\mathbf{C}}_{\mathbf{a}} + \sigma_w^2\mathbf{I}_{2N}\right)^{-1}\frac{\partial\tilde{\mathbf{C}}_{\mathbf{a}}}{\partial\alpha_l}\left(\tilde{\mathbf{C}}_{\mathbf{a}} + \sigma_w^2\mathbf{I}_{2N}\right)^{-1}\right],$$

$$J_{\sigma_w^2,\sigma_w^2} = \frac{1}{2}\mathrm{Tr}\left[\left(\tilde{\mathbf{C}}_{\mathbf{a}} + \sigma_w^2\mathbf{I}_{2N}\right)^{-2}\right],$$

$$J_{\alpha_k,\sigma_w^2} = \frac{1}{2}\mathrm{Tr}\left[\frac{\partial\tilde{\mathbf{C}}_{\mathbf{a}}}{\partial a_k}\left(\tilde{\mathbf{C}}_{\mathbf{a}} + \sigma_w^2\mathbf{I}_{2N}\right)^{-2}\right],$$

$$J_{\varphi_k,\varphi_l} = 2\pi^2\mathrm{Tr}\left[\mathbf{D}_k\left(\tilde{\mathbf{C}}_{\mathbf{a}} + \sigma_w^2\mathbf{I}_{2N}\right)\mathbf{D}_l\left(\tilde{\mathbf{C}}_{\mathbf{a}} + \sigma_w^2\mathbf{I}_{2N}\right)^{-1}\right.$$

$$+\mathbf{D}_l\left(\tilde{\mathbf{C}}_{\mathbf{a}} + \sigma_w^2\mathbf{I}_{2N}\right)\mathbf{D}_k\left(\tilde{\mathbf{C}}_{\mathbf{a}} + \sigma_w^2\mathbf{I}_{2N}\right)^{-1}$$

$$\left.-2\mathbf{D}_k\mathbf{D}_l\right]$$

$$J_{\alpha_k,\varphi_k} = i\pi\mathrm{Tr}\left\{\frac{\partial\tilde{\mathbf{R}}_{\mathbf{a}}}{\partial\alpha_k}\left[\left(\tilde{\mathbf{C}}_{\mathbf{a}} + \sigma_w^2\mathbf{I}_{2N}\right)^{-1}\mathbf{D}_k\right.\right.$$

$$\left.\left.-\mathbf{D}_k\left(\tilde{\mathbf{C}}_{\mathbf{a}} + \sigma_w^2\mathbf{I}_{2N}\right)^{-1}\right]\right\}$$

$$J_{\sigma_w^2,\varphi_k} = 0,$$

where $\mathbf{D}_k = \left[\mathbf{d}_k, \mathbf{0}_N; \mathbf{0}_N, -\mathbf{d}_k\right]$ for $k = 0,1$ with $\mathbf{d}_0 = \mathbf{I}_N$ and $\mathbf{d}_1 = \mathrm{diag}\left[(0, \cdots, N-1)\right]$. The above expressions were given in [31], and partially in [3] when $a(n)$ was circular and complex-valued. When $a(n)$ is circular and complex-valued, the term $J_{\varphi_0,\varphi_0} = 0$, which means that the constant phase is not identifiable when the pseudo-correlation is zero. Consequently, only a non-null pseudo-correlation enables us to estimate the constant phase. Apart from this comment about the constant phase, it is difficult to provide more insights with these expressions, and to distinguish the difference between the circular case and the noncircular case. We therefore now move on to the asymptotic case, i.e., for *N* sufficiently large.

3.2.2 Asymptotic Case

When *N* becomes large, we have to separately treat the circular case and the noncircular case. Let us begin with the circular case.

3.2.2.1 Circular Case

When the signal, $r(n)$, is circular, one can remark that $r(n)$ is stationary, due to our signal model given in Equation (1). This enables us to simplify the asymptotic expressions for the Fisher information matrix by applying Whittle's formula [41].

In [3], the asymptotic expressions for the Cramer-Rao bound are given for $C_a(\tau)$ real valued and positive. The latter assumption has been justified by many other authors [1, 23-25]. For instance, if $a(n)$ is associated with the Doppler-spread phenomenon, $C_a(\tau)$ often follows the Jakes model [42, 43], and thus $C_a(\tau) = \sigma_a^2 J_0(\Delta\tau)$, where σ_a^2 is the variance of $a(n)$, Δ is the Doppler spread, and $J_0(\cdot)$ is the Bessel function of first kind. In such a case, one can prove that the estimates of $[\varphi_0, \varphi_1]$ are decoupled from the other parameters, $\left[\sigma_w^2, \alpha_1, \cdots, \alpha_K\right]$. As remarked in the previous subsection, the phase, φ_0, cannot be estimated in the circular case. As a consequence, we can focus only on J_{φ_1,φ_1}. After tedious algebraic manipulations, one can find that

$$\lim_{N\to\infty}\frac{1}{N}J_{\varphi_1,\varphi_1} = \delta$$

with

$$\delta = \int_0^1\left[\frac{C_a'\left(e^{2i\pi f}\right)}{C_a\left(e^{2i\pi f}\right) + \sigma_w^2}\right]^2 df$$

and where $C_a'\left(e^{2i\pi f}\right)$ is the derivative function of $C_a\left(e^{2i\pi f}\right)$ with respect to f. As the Cramer-Rao bound is the inverse of the Fisher information matrix, we have

$$\mathrm{GCRB}(\varphi_1) \approx \frac{1}{\delta N} \text{ (circular case).}$$

We remark that the frequency can be estimated as soon as $\delta \neq 0$, i.e., as soon as the process $a(n)$ does not have a flat spectrum. We thus need to have a colored Gaussian non-constant amplitude process – and not a white Gaussian non-constant amplitude process – to be able to estimate the frequency, if the process is circular. Moreover, the Cramer-Rao bound is proportional to $1/N$, and so the minimum-achievable mean square estimation error decreases quite slowly with respect to the number of available samples.

3.2.2.2 Non-Circular Case

Unlike [3], here we cannot apply Whittle's formula [41], because $r(n)$ is not stationary with respect to its pseudo-correlation. Below, the results introduced are in fact obtained via theorems dealing with the inversion of (large) Toeplitz matrices [44, 45].

After simple but tedious calculations, the Fisher information matrix was found in [31] to be

$$\lim_{N\to\infty} \frac{1}{N} J_{\alpha_k,\alpha_l} = \frac{1}{2}\theta_{k,l},$$

$$\lim_{N\to\infty} \frac{1}{N} J_{\sigma_w^2,\sigma_w^2} = \frac{1}{2}\gamma,$$

$$\lim_{N\to\infty} \frac{1}{N} J_{\alpha_k,\sigma_w^2} = \frac{1}{2}\beta_k,$$

$$\lim_{N\to\infty} \frac{1}{N} J_{\varphi_0,\varphi_0} = 16\pi^2\xi,$$

$$\lim_{N\to\infty} \frac{1}{N^3} J_{\varphi_1,\varphi_1} = \frac{16\pi^2}{3}\xi,$$

$$\lim_{N\to\infty} \frac{1}{N^2} J_{\varphi_0,\varphi_1} = 8\pi^2\xi,$$

$$\lim_{N\to\infty} \frac{1}{N} J_{\alpha_k,\varphi_0} = 4\pi\mu_k,$$

$$\lim_{N\to\infty} \frac{1}{N^2} J_{\alpha_k,\varphi_1} = 2\pi\mu_k,$$

where

$$\theta_{k,l} = \int_0^1 \frac{1}{X\left(e^{2i\pi f}\right)^2} \frac{\partial X\left(e^{2i\pi f}\right)}{\partial \alpha_k} \frac{\partial X\left(e^{2i\pi f}\right)}{\partial \alpha_l} df$$

$$+\int_0^1 \frac{1}{X\left(e^{2i\pi f}\right)} \left[Q_{k,l}^{(P_a)}\left(e^{2i\pi f}\right) - Q_{k,l}^{(C_a+\sigma_w^2)}\left(e^{2i\pi f}\right) \right] df$$

$$\gamma = \int_0^1 \frac{1}{X\left(e^{2i\pi f}\right)^2} \left\{ \left[C_a\left(e^{2i\pi f}\right) + \sigma_w^2 \right]^2 \right.$$

$$\left. + \left[\underline{C_a}\left(e^{2i\pi f}\right) + \sigma_w^2 \right]^2 + 2\underline{P_a}\left(e^{2i\pi f}\right) P_a\left(e^{2i\pi f}\right) \right\} df$$

$$\beta_k = \int_0^1 \frac{1}{X\left(e^{2i\pi f}\right)} \frac{\partial X\left(e^{2i\pi f}\right)}{\partial \alpha_k} df$$

$$\mu_k = \Im m\left[\int_0^1 \frac{\underline{P_a}\left(e^{2i\pi f}\right)}{X\left(e^{2i\pi f}\right)} \frac{\partial P_a\left(e^{2i\pi f}\right)}{\partial \alpha_k} df \right]$$

$$\xi = \int_0^1 \frac{P_a\left(e^{2i\pi f}\right) \underline{P_a}\left(e^{2i\pi f}\right)}{X\left(e^{2i\pi f}\right)} df$$

with

$$\underline{\nu}\left(e^{2i\pi f}\right) = \overline{\nu\left(e^{-2i\pi f}\right)},$$

$$Q_{k,l}^{(\nu)}\left(e^{2i\pi f}\right)$$

$$= \frac{\partial \nu\left(e^{2i\pi f}\right)}{\partial \alpha_k}\frac{\partial \underline{\nu}\left(e^{2i\pi f}\right)}{\partial \alpha_l} + \frac{\partial \underline{\nu}\left(e^{2i\pi f}\right)}{\partial \alpha_k}\frac{\partial \nu\left(e^{2i\pi f}\right)}{\partial \alpha_l}$$

$$X\left(e^{2i\pi f}\right) = \left[C_a\left(e^{2i\pi f}\right) + \sigma_w^2\right]\left[\underline{C_a}\left(e^{2i\pi f}\right) + \sigma_w^2\right]$$

$$- P_a\left(e^{2i\pi f}\right)\underline{P_a}\left(e^{2i\pi f}\right)$$

We next study different scenarios. First, we consider the case where the receiver knows $\left[\sigma_w^2, \alpha_1, \cdots, \alpha_K\right]$, i.e., the statistics of multiplicative and additive noise. In this case, the Gaussian Cramer-Rao bounds result from the inverse of the 2×2 Fisher information matrix

$$\mathbf{J}_{[\varphi_0,\varphi_1]} = \begin{bmatrix} J_{\varphi_0,\varphi_0} & J_{\varphi_0,\varphi_1} \\ J_{\varphi_0,\varphi_1} & J_{\varphi_1,\varphi_1} \end{bmatrix}.$$

This yields

$$\mathrm{GCRB}\left(\varphi_0\right)_{|\text{noise statistics known}} = \frac{1}{4\pi^2 \xi N}$$

and

$$\mathrm{GCRB}\left(\varphi_1\right)_{|\text{noise statistics known}} = \frac{3}{4\pi^2 \xi N^3}.$$

Second, in the case where $\left[\sigma_w^2, \alpha_1, \cdots, \alpha_K\right]$ are unknown at the receiver, we obtain (see [31])

$$\mathrm{GCRB}\left(\varphi_0\right)_{|\text{noise statistics unknown}}$$

$$= \mathrm{GCRB}\left(\varphi_0\right)_{|\text{noise statistics known}} + \frac{m}{16\pi^2 \xi^2 N}.$$

Here, m is a bounded scalar taking the following form:

$$m = \boldsymbol{\mu}^{\mathrm{T}}\left[\boldsymbol{\theta}/2 - \boldsymbol{\mu}\boldsymbol{\mu}^{\mathrm{T}}/\xi - \boldsymbol{\beta}\boldsymbol{\beta}^{\mathrm{T}}/(2\gamma)\right]^{-1}\boldsymbol{\mu}$$

where

$$\boldsymbol{\theta} = (\theta_{k,l})_{1\le k,l\le K},$$

$$\boldsymbol{\beta} = (\beta_k)_{1\le k\le K},$$

$$\boldsymbol{\mu} = (\mu_k)_{1\le k\le K}.$$

Using the previous expressions for the asymptotic Cramer-Rao bound, we make the following comments:

- The convergence rates for the phase and frequency estimations are $1/N$ and $1/N^3$, respectively, regardless of the color of the multiplicative noise. Recall that for circular complex-valued processes, the phase is not identifiable, and the frequency is identifiable only if the multiplicative noise is colored, with a convergence rate of $1/N$. Notice that a real-valued process can be viewed as a specific case of a noncircular complex-valued process where the imaginary part is zero. Consequently, in terms of performance, the main cutoff is not complex/real, but circular/noncircular.

- We recall that the Cramer-Rao bound associated with the "pure" frequency-estimation issue (i.e., only disturbed by a constant amplitude) is proportional to $1/N^3$ [46]. Consequently, thanks to the non-circularity property of the non-constant amplitude, the non-constant amplitude does not lead to a significant loss in performance.

- Surprisingly, the same frequency-estimation performance is obtained whether the statistics of $a(n)$ are known or not.

- The frequency-estimation performance depends only on ξ, which refers to an information rate provided by the non-circularity. Indeed, the performance improves when ξ increases.

- In the noiseless case, we observe a floor effect (i.e., $\mathrm{CRB}(\varphi_1) \neq 0$ when $\sigma_w^2 = 0$). This effect vanishes if $C_a\left(e^{2i\pi f}\right)C_a\left(e^{-2i\pi f}\right) = P_a\left(e^{2i\pi f}\right)P_a\left(e^{-2i\pi f}\right)$. This condition is fulfilled, for example, when the multiplicative noise is real-valued.

As a conclusion, we remind the reader that the Gaussian Cramer-Rao bound is of interest in many applications: Doppler radar, direction-of-arrival estimation, and digital communication over Rayleigh flat-fading channels. If the non-constant amplitude is non-Gaussian, the Gaussian Cramer-Rao bound is not a lower bound for the estimation problem anymore. Nevertheless, it is still of interest, since the Gaussian Cramer-Rao bound is a lower bound for any second-order-based estimator (well-adapted to, e.g., digital BPSK modulation) [47]. Consequently, the

Gaussian Cramer-Rao indicates what is the best expected performance if we carry out an estimator based only on mean and correlation.

Actually, in the non-Gaussian case, the non-circularity may also play a significant role. For example, if $a(n)$ is assumed to belong to a QAM modulation, $a(n)$ is circular at second order (i.e., $\mathbb{E}\left[a(n)a(n)\right]=0$, but is non-circular at fourth order ($\mathbb{E}\left[a(n)a(n)a(n)a(n)\right]\neq 0$). Thanks to this fourth-order non-circularity, we are able to build an estimator for which the mean-square estimation error is proportional to $1/N^3$, and not $1/N$ [47, 48]. This is not in contradiction with the previous results, since a QAM modulation is not Gaussian, and so the high-order statistics of $a(n)$ strongly help to improve the estimation performance.

4. Deriving the Modified Cramer-Rao Bound

To overcome the complexity concern of deriving the true Cramer-Rao bound[1] in the non-Gaussian case, it is possible to define other lower-Cramer-Rao-bound-like bounds that are easier to compute but less tight than the true bound. The most well-spread is the so-called *modified* Cramer-Rao bound (MCRB) [9, 10]. Once again, we will restrict our analysis to the estimation of $\mathbf{u}=[\varphi_0,\varphi_1]$. The elements of the *modified* Fisher information matrix (MFIM) are then defined as follows:

$$\mathcal{J}_{\varphi_k,\varphi_l}=\mathbb{E}_{\mathbf{a}}\left[\frac{\partial \ln p(\mathbf{r}\,|\,\mathbf{u},\mathbf{a})}{\partial\varphi_k}\frac{\partial \ln p(\mathbf{r}\,|\,\mathbf{u},\mathbf{a})}{\partial\varphi_l}\right].$$

After standard algebraic manipulations, we obtain

$$\mathcal{J}_{\varphi_k,\varphi_l}=\frac{8\pi^2}{\sigma_w^2}\mathbb{E}_{\mathbf{a}}\left[\mathbf{a}\mathbf{d}_k\mathbf{d}_l\mathbf{a}^{\mathrm{H}}\right].$$

For large N, the resulting modified Cramer-Rao bounds were given in [9, 10]. We have

$$\mathrm{MCRB}(\varphi_0)\approx\frac{\left[(k_0+N-1)^3-(k_0)^3\right]\sigma_w^2}{2\pi^2c_a(0)N^4}$$

and

$$\mathrm{MCRB}(\varphi_1)\approx\frac{3\sigma_w^2}{2\pi^2c_a(0)N^3}.$$

We note that in the case of linear modulation it was assumed that $c_a(0)=1$, such that the above modified Cramer-Rao bounds, for N large and odd valued and $k_0=(N-1)/2$, reduce to the Cramer-Rao bounds from Equations (13) and (14) upon the factor $R_\Omega(\sigma_w^{-2})$ from Equation (15). We have the following comments:

- The derivation of the modified Cramer-Rao bounds is very easy and enables us to obtain simple closed-form expressions.
- These expressions seem to be "too" simple and do not provide a lot of information, since the Cramer-Rao bound does not depend on the nature of $a(n)$ (circular/noncircular in the Gaussian case, channel code and symbol constellation in the non-Gaussian case), while we have seen before that this is crucial information (see the previous discussion in the Gaussian case and the asymptotic Cramer-Rao-bound expressions in non-Gaussian case).
- Nevertheless, the modified Cramer-Rao bound can sometimes be of great interest. Indeed, if $a(n)$ belongs to a finite set of symbol constellation points Ω, the true Cramer-Rao bound (for which no explicit expressions are available) is well approximated by the modified Cramer-Rao bound at high SNR [11].
- An unexpected consequence of the previous remark is the following. Let us consider the modified Cramer-Rao bound for estimating the frequency offset in the case of digital communication using a BPSK symbol constellation set, i.e., $a(n)$ takes values in the set $\{-1,1\}$ which implies that $L=2$ and $f_L=c_a(0)=1$. We have

$$\mathrm{MCRB}(\varphi_1)_{\mathrm{BPSK}}\approx\frac{3\sigma_w^2}{2\pi^2N^3}.$$

Due to the previous item, there is equivalence between MCRB and ACRB at high SNR for BPSK. We therefore know that

$$\mathrm{ACRB}(\varphi_1)_{|\text{high SNR,BPSK}}=\frac{3\sigma_w^2}{2\pi^2N^3}$$

and, thanks to Equation (16), we get

$$\mathrm{ACRB}(\varphi_1)_{|\text{low SNR,BPSK}}=\frac{3\sigma_w^4}{4\pi^2N^3}.$$

Obviously, at low SNR, the true Cramer-Rao bound for BPSK starts to seriously deviate from the modified Cramer-Rao bound.

If we inspect the Gaussian Cramer-Rao bound for uncorrelated and real-valued Gaussian $a(n)$, we obtain

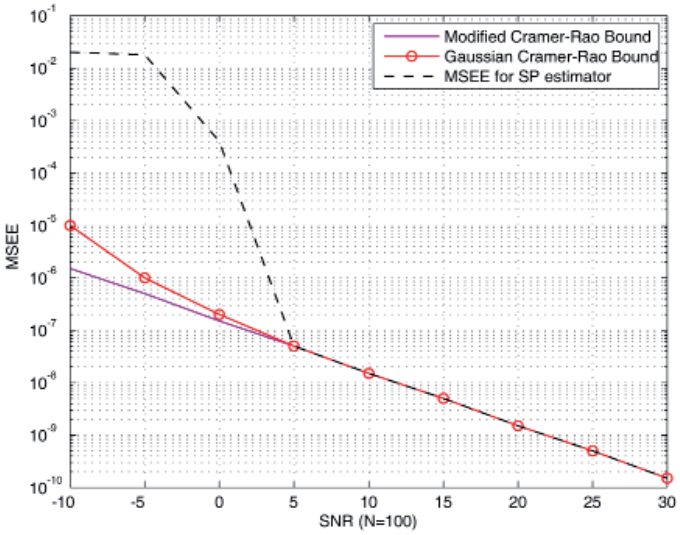

Figure 1. The modified Cramer-Rao bound (MCRB), Gaussian Cramer-Rao bound (GCRB), and mean-square estimation error (MSEE) for the square-power estimator as a function of the SNR.

$$\mathrm{GCRB}(\varphi_1) = \frac{3\left[2\sigma_w^2 + \sigma_w^4\right]}{4\pi^2 N^3}.$$

Surprisingly, the Gaussian Cramer-Rao bound predicts the performance of a BPSK based non-constant amplitude well for both low *and* high SNR, whereas a BPSK constellation is not Gaussian at all! Consequently, the Gaussian Cramer-Rao bound is a powerful tool for analyzing the frequency mean-square estimation error in the BPSK context, whereas the modified Cramer-Rao bound is not (except at high SNR).

5. Deriving the Barankin Bound

Let us reconsider the signal model given in Equation (1), with $k_0 = 0$ and $a(n)$ a zero-mean Gaussian stationary process with correlation $c_a(\tau)$ and pseudo-correlation $p_a(\tau)$. For the sake of simplicity, we further assume that the noise statistics, i.e., $\{c_a(\tau), p_a(\tau)\}_{\tau\in\mathbb{Z}}$ and σ_w^2, are known at the receiver. This assumption was made in [49], and was partially made in [28], for deriving Barankin bounds (BB) because the computational and analytical complexities are otherwise too high. It can also be noted that the Cramer-Rao bound for frequency estimation is insensitive to the knowledge of the noise statistics as soon as the number of samples is large enough (see [31] and the Gaussian-Cramer-Rao-bound discussion above). We thus can expect that the error induced by neglecting the estimation step with respect to the noise statistics will be sufficiently small so that our further conclusions still hold in the case of unknown noise statistics.

To well understand the interest of bounds other than the Cramer-Rao bound, let us consider the following

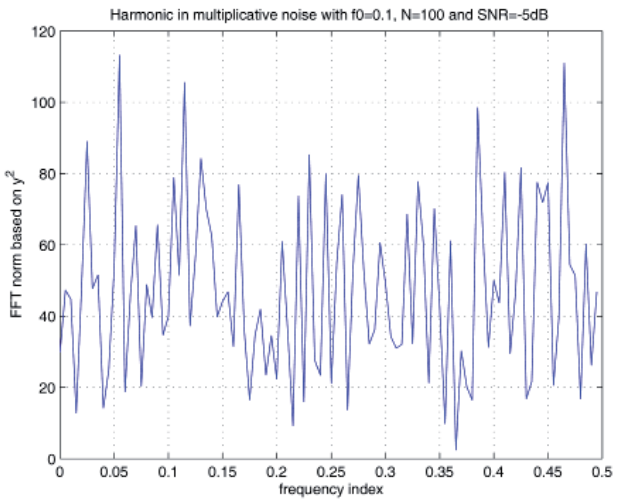

Figure 2a. The cost function $F(\varphi)$ as a function of φ for SNR = −5 dB.

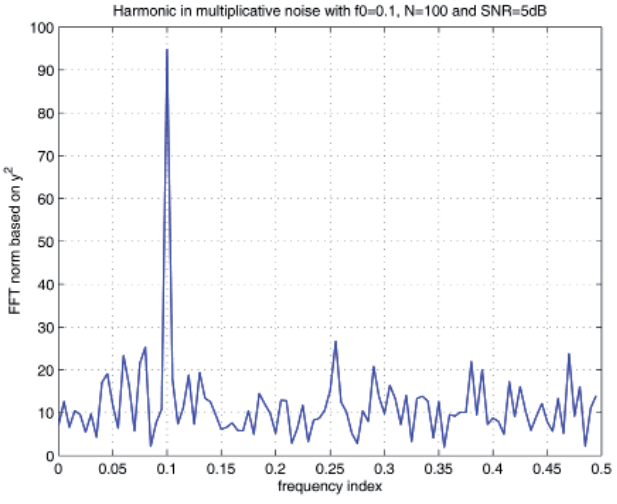

Figure 2b. The cost function $F(\varphi)$ as a function of φ for SNR = 5 dB.

example. The signal model is the model from Equation (1) with $a(n)$ a real-valued Gaussian process. To estimate the frequency, as $a(n)$ is noncircular (since real-valued), one can use the so-called square-power estimator [47], defined as follows:

$$\hat{\varphi}_1 = \arg\max_{\varphi} \underbrace{\left| \frac{1}{N} \sum_{n=0}^{N-1} r(n)^2 \, e^{-2j\pi(2\varphi)n} \right|^2}_{F(\varphi)} .$$

In Figure 1, we plot the mean-square estimation error of this estimator, and the modified and Gaussian Cramer-Rao bound, as functions of the SNR, when $N = 100$. We observed that at high SNR, the estimator was powerful and even efficient (the mean-square estimation error equals the Cramer-Rao bound). In contrast, at low SNR, there was a large mismatch between the mean-square estimation error and the Cramer-Rao bound. The question is, is the considered estimator not relevant at low SNR, or is the Cramer-Rao bound not tight enough at low SNR? We will show that the Cramer-Rao bound is not tight enough. To demonstrate that, we introduce other lower bounds on the mean-square estimation error that are much tighter at low SNR than the Cramer-Rao bound.

We can now attempt to understand why the Cramer-Rao bound is not tight enough at low SNR. In Figure 2, we plot the cost function, $F(\cdot)$, of the square-power estimator for $\mathrm{SNR} = -5$ dB (Figure 2a) and for $\mathrm{SNR} = 5$ dB (Figure 2b). The frequency sought is $\varphi_1 = 0.1$. We remark that at high SNR, the peak around the true value of the frequency was well detected, whereas at low SNR, there was a mis-detection of the peak, which significantly degraded the performance. Consequently, the performance degradation was due to a higher peak far away from the true frequency. These "bad" realizations are called "outliers." By inspecting in detail the Fisher information matrix from Equation (3), we remark that it depends on the behavior of the likelihood function around the true frequency, since the derivative functions involved are calculated at the true frequency. The Cramer-Rao bound is therefore unable to take into account the mis-detection of the peak, and automatically assumes a correct detection of the peak, even if it is wrong. At low SNR (when the mis-detection of the peak occurs), the Cramer-Rao bound is thus truly too optimistic.

We are now interested in another bound that inspects the likelihood function around the true frequency, but not only there. We therefore introduce the following set of so-called "test-points,"

$$\left\{ \phi(k) = \left[\phi_0(k), \phi_1(k) \right]^{\mathrm{T}} \right\}_{1 \le k \le n},$$

at which the likelihood function will be evaluated. We are now able to define the Barankin bound of order p as follows:

$$\mathrm{BB}_p(\varphi_0, \varphi_1) = \sup_{\mathcal{E}} S_p(\mathcal{E}),$$

where

$$S_p(\mathcal{E}) = \mathcal{E}\left[\mathbf{B}(\mathcal{E}) - \mathbf{1}_p \mathbf{1}_p^{\mathrm{T}} \right]^{-1} \mathcal{E}^{\mathrm{T}},$$

with

$$\mathcal{E} = \left[\phi(1) - \mathbf{u}^{\mathrm{T}}, \ldots, \phi(p) - \mathbf{u}^{\mathrm{T}} \right]$$

and

$$\mathbf{1}_p = \mathrm{ones}(p,1).$$

The term sup stands for the smallest upper bound on the set $\mathcal{E}$. Furthermore, $\mathbf{B}(\mathcal{E}) = \left(B_{k,l} \right)_{1 \le k,l \le p}$ is the following $p \times p$ matrix:

$$B_{k,l} = \mathbb{E}\left\{ L\left[\mathbf{r}, \mathbf{u}, \phi(k) \right] L\left[\mathbf{r}, \mathbf{u}, \phi(l) \right] \right\},$$

with

$$L\left[\mathbf{r}, \mathbf{u}, \phi(k) \right] = \frac{p\left[\mathbf{r} \mid \phi(k) \right]}{p(\mathbf{r} \mid \mathbf{u})}.$$

The mean-square estimation error of any unbiased estimator is greater than the Barankin bound of any order p ([40]). From an asymptotic point of view (as $p \to \infty$), the Barankin bound is even the tightest lower bound that one can find [27, 28]. As for the choice of the test points, it is usual to consider the following structure for $\mathcal{E}$ [28, 29]:

$$\mathcal{E} = \begin{bmatrix} \phi_0 - \varphi_0 & 0 \\ 0 & \phi_1 - \varphi_1 \end{bmatrix} = \mathrm{diag}(\varepsilon_0, \varepsilon_1). \qquad (17)$$

Our main concern hereafter is to derive a closed-form expression for the matrix $\mathbf{B}$ for such test points.

Let us now remind the reader of some notation. The covariance matrix $\tilde{\mathbf{C}}_{\mathbf{r}}(\phi)$ of the multivariate process $\tilde{\mathbf{r}}$ can be written as follows:

$$\tilde{\mathbf{C}}_{\mathbf{r}}(\phi) = \tilde{\mathbf{S}}(\phi) \left(\tilde{\mathbf{C}}_{\mathbf{a}} + \sigma_w^2 \mathbf{I}_{2N} \right) \tilde{\mathbf{S}}^{\mathrm{H}}(\phi), \qquad (18)$$

where

$$\tilde{\mathbf{S}}(\phi) = \begin{bmatrix} \mathbf{S}(\phi) & \mathbf{0}_N \\ \mathbf{0}_N & \overline{\mathbf{S}}(\phi) \end{bmatrix}.$$

After straightforward algebraic manipulations, we finally obtain

$$B_{k,l} = \begin{cases} \dfrac{1}{\sqrt{\det\left(\mathbf{Q}_{k,l}\right)}} & \text{if } \mathbf{Q}_{k,l} > 0 \\ +\infty & \text{otherwise} \end{cases},$$

with

$$\mathbf{Q}_{k,l} = \left\{\tilde{\mathbf{C}}_{\mathbf{r}}\left[\phi(k)\right]^{-1} + \tilde{\mathbf{C}}_{\mathbf{r}}\left[\phi(l)\right]^{-1}\right\}\tilde{\mathbf{C}}_{\mathbf{r}}(\mathbf{u}) - \mathbf{I}_{2N}.$$

These expressions were introduced in [49] and [28] in a slightly different form (due to the circularity assumption on the non-constant amplitude), and in [31] for the general case.

We now just focus on our main parameter of interest: the frequency, φ_1. For the standard test points described in Equation (17), the Barankin bound for φ_1 takes the following form [28]:

$$\mathrm{BB}(\varphi_1) = \sup_{\varepsilon_0,\varepsilon_1} \frac{\varepsilon_1^2}{\left(B_{1,1}-1\right) - \dfrac{\left(B_{0,1}-1\right)^2}{B_{0,0}-1}}.$$

The term $\left(B_{0,1}-1\right)^2 / \left(B_{0,0}-1\right)$ represents the loss in performance due to joint phase and frequency-parameter estimation.

We remark that strictly speaking, the Barankin bound is not obtained in closed form, since the maximum operator still occurs. Nevertheless, the existing expressions enable us to very quickly compute the Barankin bound.

As we will see in the simulation section, the Barankin bound enables us to partially predict the outliers effect, i.e., the mismatch between the Cramer-Rao bound and the real estimator's performance. Consequently the poor estimation performance of the standard square-power estimator (well adapted to BPSK or a real-valued Gaussian process) is shown to be connected to the poor tightness of the Cramer-Rao bound. Decreasing the gap between the Cramer-Rao bound and the estimator performance for a given number of samples at very low SNR is thus impossible. The Cramer-Rao bound is too optimistic in such a context, and has to be replaced with the Barankin bound.

6. Deriving the Ziv-Zakai Bound

To analyze the mismatch between the Cramer-Rao bound and the real estimator's performance, we have considered the so-called Barankin bound in the previous section. Even though this Barankin bound is much tighter than the Cramer-Rao bound and roughly predicts the outliers effect, there is still a mismatch between bound and estimator performance. In this section, we will therefore introduce a third, much-more-powerful bound, the Ziv-Zakai bound (ZZB).

We note that the Ziv-Zakai bound needs a new paradigm on the parameters sought: the Bayesian approach. Unlike what was previously done, we have to consider the parameters sought as a realization of a random variable. This random variable is further described by a distribution, which characterizes the *a priori* information available on the parameters sought. For instance, for frequency-offset estimation, we only know that the frequency is normalized, and thus it may uniformly take values in the interval $[-1/2, 1/2]$.

In [20, 50], it was proven that the following inequality holds for any vector $\mathbf{z} = [z_0, z_1]$:

$$\mathbf{z}\mathbf{E}_{\mathbf{u}}\mathbf{z}^{\mathrm{T}} \geq \int_0^{\infty} \Delta \left[\max_{\substack{(\varepsilon_0,\varepsilon_1) \\ z_0\varepsilon_0 + z_1\varepsilon_1 = \Delta}} f(\varepsilon_0,\varepsilon_1) \right] d\Delta, \quad (19)$$

where $\mathbf{E}_{\mathbf{u}}$ denotes the error-correlation matrix related to the estimation of a random variable $\mathbf{u} = [\varphi_0, \varphi_1]$, and

$$f(\varepsilon_0,\varepsilon_1) = \int \min\left[p(\mathbf{u}), p(\mathbf{u}+\varepsilon)\right] P_e(\mathbf{u}, \mathbf{u}+\varepsilon)\, d\mathbf{u}, \quad (20)$$

with $\varepsilon = [\varepsilon_0, \varepsilon_1]$.

The function $p(\mathbf{u})$ is the a priori density function of the bivariate parameter $\mathbf{u}$, and $P_e(\mathbf{u}, \mathbf{u}+\varepsilon)$ is the error probability when the optimal detector (namely, the ML detector) is used to decide between the following two hypotheses:

$$\begin{cases} H_0 : y(n) = a(n) e^{2i\pi(\varphi_0 + \varphi_1 n)} + w(n) \\ H_1 : y(n) = a(n) e^{2i\pi\left[(\varphi_0+\varepsilon_0) + (\varphi_1+\varepsilon_1)n\right]} + w(n) \end{cases}$$

where hypotheses H_0 and H_1 are equally likely.

The right-hand side of Equation (19) is called the Ziv-Zakai bound. By inspecting Equation (19), one can remark that the likelihood of $\mathbf{u}$ is scanned over the entire search interval of $\mathbf{u}$, as is also the case for the Barankin bound [31]. Once again, this contrasts with the Cramer-Rao bound, where the likelihood function is only evaluated around the true point. We therefore expect that the Ziv-Zakai bound can predict the outliers effect at low SNR.

Let us focus now on the Ziv-Zakai bound for φ_1, which is obtained by setting $\mathbf{z} = [0, 1]$. Therefore,

$$\mathrm{ZZB}(\varphi_1) = \int_0^{\infty} \varepsilon_1 \left[\max_{\varepsilon_0} f(\varepsilon_0, \varepsilon_1) \right] d\varepsilon_1 .$$

Actually, the mean-square estimation error of any (even biased) estimator for the frequency is greater than the $\mathrm{ZZB}(\varphi_1)$ [20].

The key task now is to express the function $f(\cdot)$ in closed form. After some simple derivations, one can see that $P_e(\mathbf{u}, \mathbf{u}+\varepsilon)$ is independent of $\mathbf{u}$, so that it can be denoted by $P_e(\varepsilon_0, \varepsilon_1)$. As a consequence, we have [50]

$$f(\varepsilon_0, \varepsilon_1) = g(\varepsilon_0, \varepsilon_1) P_e(\varepsilon_0, \varepsilon_1),$$

where

$$g(\varepsilon_0, \varepsilon_1) = \int \min\left[p(\mathbf{u}), p(\mathbf{u}+\varepsilon) \right] d\mathbf{u} .$$

Since we have no a priori information on $\mathbf{u}$, we assume that φ_0 and φ_1 are uniformly distributed over $[0, 1/2]$, i.e., the a priori distribution of the parameters of interest $p(\mathbf{u})$ is flat. We consider the interval $[0, 1/2]$ rather than $[-1/2, 1/2]$ because the phase and the frequency can only be estimated modulo $1/2$ when multiplicative noise occurs [50]. Consequently,

$$g(\varepsilon_0, \varepsilon_1) = (1/2 - \varepsilon_0)(1/2 - \varepsilon_1).$$

This leads to

$$\mathrm{ZZB}(\varphi_1)$$

$$= \int_0^{1/2} (1/2 - \varepsilon_1) \varepsilon_1 \max_{\varepsilon_0} \left[(1/2 - \varepsilon_0) P_e(\varepsilon_0, \varepsilon_1) \right] d\varepsilon_1 .$$

The rest of the section deals with the evaluation of $P_e(\varepsilon_0, \varepsilon_1)$. After tedious algebraic derivations that can be found in [53], we have

$$P_e(\varepsilon_0, \varepsilon_1) = \mathrm{Prob}\left[\sum_{n=m}^{2N-1} \lambda_n^{(+)} v_n^2 < \sum_{n=0}^{m-1} \lambda_n^{(-)} v_n^2 \right], \quad (21)$$

where

- $\{v_n\}$ is a real-valued i.i.d. (independent identically distributed) Gaussian random process with zero mean and unit variance.
- The $-\lambda_n^{(-)}$ for $n = 0, \cdots, m-1$ (with $\lambda_n^{(-)} > 0$) are the m negative eigenvalues, and $\lambda_n^{(+)} \geq 0$ for $n = m, \cdots, 2N-1$ are the positive or null eigenvalues of the $2N \times 2N$ matrix $\mathbf{T}(\varepsilon)$, defined as follows:

$$\mathbf{T}(\varepsilon) = \left[\breve{\mathbf{C}}_{\mathbf{r}}(\varepsilon)^{-1} - \breve{\mathbf{C}}_{\mathbf{r}}(0)^{-1} \right] \breve{\mathbf{C}}_{\mathbf{r}}(0),$$

where $\breve{\mathbf{C}}_{\mathbf{r}}(\varepsilon) = \mathbb{E}\left[\breve{\mathbf{r}}^{\mathrm{T}} \breve{\mathbf{r}} \right]$ with $\breve{\mathbf{r}} = \{\Re[\mathbf{r}], \Im[\mathbf{r}]\}$ and $\mathbf{r}$ is the received signal disturbed by phase ε_0 and frequency ε_1.

We now wish to derive a closed-form expression for the following term:

$$P_e(\varepsilon_0, \varepsilon_1) = \mathrm{Prob}(p_+ < p_-), \quad (22)$$

where $p_{\pm} = \sum \lambda_n^{(\pm)} v_n^2$ is a weighted sum of squared independent Gaussian variables. Notice that by construction, p_+ and p_- are independent.

If $\lambda_n^{(+)} = \lambda^{(+)}$ (respectively, $\lambda_n^{(-)} = \lambda^{(-)}$) for all corresponding n, then p_+ (respectively, p_-) obeys a χ^2 distribution with $(2N-m)$ (respectively, m) degrees of freedom. However, if the weighting coefficients are different, the $p_{\pm}$ s are not χ^2 distributed anymore. Further, expressing the distribution of $p_{\pm}$ in closed form is not tractable. Nevertheless, it can be well approximated by means of the Gamma distribution [51]. We recall that the Gamma distribution, denoted $\mathcal{G}(\aleph, \wp)$, is defined as follows:

$$P_{\aleph,\wp}(x) = \frac{x^{\aleph-1}}{\Gamma(\aleph)\wp^{\aleph}} e^{-x/\wp},$$

where $\Gamma(\cdot)$ is the Gamma function.

Hence, the distribution of $p_{\pm}$ is next approximated by the Gamma distribution, the first and second moments of which are equal to those of $p_{\pm}$. We thus obtain

$$p_+ \sim \mathcal{G}(\aleph_+, \wp_+)$$

and

$$p_- \sim \mathcal{G}(\aleph_-, \wp_-),$$

with

$$\aleph_+ = \frac{1}{2} \frac{\left[\sum_{n=m}^{2N-1} \lambda_n^{(+)} \right]^2}{\sum_{n=m}^{2N-1} \lambda_n^{(+)2}}$$

and

$$\wp_+ = 2 \frac{\sum_{n=m}^{2N-1} \lambda_n^{(+)2}}{\sum_{n=m}^{2N-1} \lambda_n^{(+)}},$$

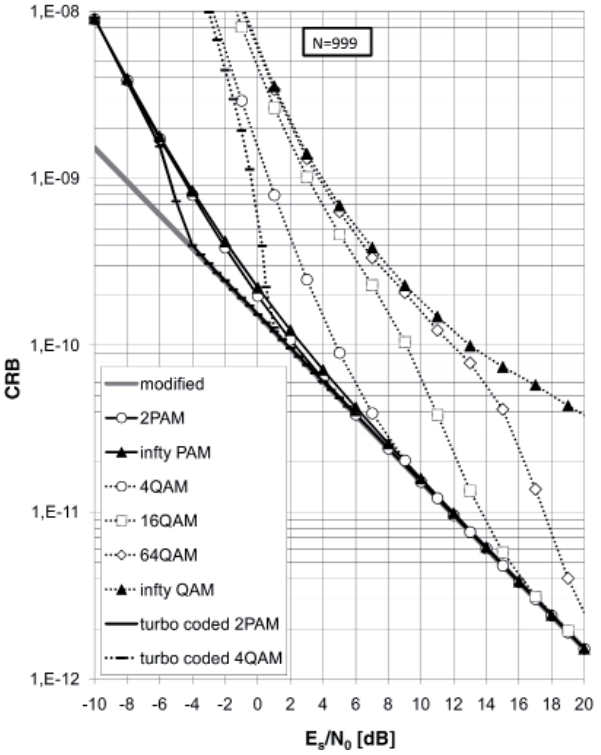

Figure 3. The Cramer-Rao bounds related to the estimation of φ_1 resulting from the observation model, Equation (1), as a function of the SNR, E_s/N_0, for random, linear, MPAM, and MQAM, coded and uncoded, modulations.

and

$$\aleph_- = \frac{1}{2}\frac{\left[\sum_{n=0}^{m-1}\lambda_n^{(-)}\right]^2}{\sum_{n=0}^{m-1}\lambda_n^{(-)2}}$$

and

$$\wp_- = 2\frac{\sum_{n=0}^{m-1}\lambda_n^{(-)2}}{\sum_{n=0}^{m-1}\lambda_n^{(-)}}.$$

As $p_\pm$ is now assumed Gamma distributed, Equation (22) can be simplified. Indeed, by using the fact that the square root of a Gamma-distributed random variable is Nakagami distributed, and by using Equation (46) in [52], we have that

$$P_e(\varepsilon_0,\varepsilon_1) = \left(\frac{\wp_+}{\wp_-}\right)^{\aleph_+}\frac{\Gamma(\aleph_+ + \aleph_-)}{\aleph_+\Gamma(\aleph_+)}$$

$$\cdot\ {}_2F_1\left(\aleph_+ + \aleph_-, \aleph_+, \aleph_+ + 1; -\frac{\wp_+}{\wp_-}\right),$$

where ${}_2F_1(\cdot)$ is the hypergeometric function.

The above expression for $P_e(\varepsilon_0,\varepsilon_1)$ represents the main available result on the Ziv-Zakai bound derivations [53]. Although this expression is not interpretable, its numerical computation will provide interesting results, as seen below. Notice also that the expressions obtained for the Ziv-Zakai bound are not anymore a bound, strictly speaking, since we are not able to prove that the approximate expressions are less than the exact (but unavailable) bound. However, by checking the approximation numerically, we have observed that the approximation is very tight.

7. Simulation Results

7.1 Non-Constant Complex Amplitude = Digital Data Symbol

Figure 3 presents some numerical results for the true Cramer-Rao bound regarding the estimation of the frequency offset from the observation of $N = 999$ linearly modulated signal samples that were obtained by means of computer simulations. The following signaling constellations, Ω, were considered:

- *M*-ary *pulse-amplitude modulation*} (*M*-PAM) for which

$$\Omega = \sqrt{\frac{3}{\left(M^2-1\right)}}\mathcal{I}_M .$$

- *M*-ary *quadrature-amplitude modulation* (*M*-QAM) for which

$$\Omega = \left\{\omega : \Re\{\omega\}, \Im\{\omega\} \in \sqrt{\frac{3}{2(M-1)}}\mathcal{I}_{\sqrt{M}}\right\},$$

where $\Re\{\cdot\}$ and $\Im\{\cdot\}$ denote the real and the imaginary parts of a complex number.

In the above,

$$\mathcal{I}_m = \{\pm 1, \pm 3, ..., \pm(m-1)\}. \qquad (23)$$

We further considered uncoded and turbo-coded linear modulation. The turbo-coded transmission scheme encompasses the parallel concatenation of two identical binary 16-state rate-1/2 recursive systematic convolutional encoders, with generator polynomials $(21)_8$ and $(37)_8$ in octal notation, via a pseudo-random interleaver with block length N_b information bits. An appropriate puncturing pattern, so that the block at the turbo-encoder output comprises N_c coded bits, was used. This binary turbo code was followed by conventional Gray-mapped 2PAM or

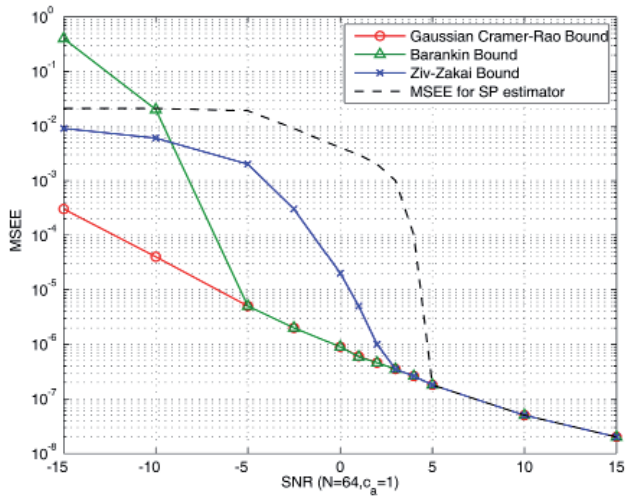

Figure 4. The mean-square estimation error as a function of the SNR.

4QAM modulation, giving rise to a block of N random data symbols, with $N = N_c = 3N_b$ for the case 2PAM, and $N = N_c/2 = N_b$ for the case of 4QAM.

Our simulation results confirmed that the high-SNR limit of the Cramer-Rao bounds equals the modified Cramer-Rao bound. Comparing the Cramer-Rao bounds for coded and uncoded transmission, we observed that for a given constellation type, they were equal at sufficiently high SNRs. However, at lower SNRs there was a gap between the Cramer-Rao bounds for coded and uncoded transmissions. When E_s/N_0 decreased, a point $(E_s/N_0)_{thr}$ was reached where the Cramer-Rao bounds started to diverge from their high-SNR limit. For coded transmission, $(E_s/N_0)_{thr}$ corresponded to a coded BER (bit-error rate) of about 10^{-3}. For uncoded transmission, $(E_s/N_0)_{thr}$ corresponded to an uncoded BER of about 10^{-3}, and consequently exceeded $(E_s/N_0)_{thr}$ for coded transmission by an amount equal to the coding gain.

For uncoded transmission, the following observations can further be made:

- For both constellation types (PAM, QAM), we observed that for a given value of E_s/N_0, the Cramer-Rao bound increased with M, which indicated that for the larger constellations, carrier recovery was inherently harder to accomplish. This effect was clearly evident for MQAM, in which case the curves corresponding to large M exhibited an almost horizontal portion, but was almost unnoticeable for MPAM. Figure 3 also shows the limiting curve for M approaching infinity. This situation corresponded to data symbols that were continuous random variables, that were uniformly distributed in the interval $\left[-\sqrt{3},\sqrt{3}\right]$ for PAM, and in a square with side $\sqrt{6}$ for QAM. In the case of infinite-size constellations, the Cramer-Rao bounds do not necessarily converge to the corresponding modified Cramer-Rao bounds for large SNR, according to [11]. This is due to the non-diagonal nature of the Fisher information matrix, related to the joint likelihood function $p(\mathbf{r}|\mathbf{a},\mathbf{u})$ of $\mathbf{a}$ and $\mathbf{u}$, with $\mathbf{u} = [\varphi_0, \varphi_1]$.
- For finite M, the Cramer-Rao bound does converge to the modified Cramer-Rao bound when E_s/N_0 is

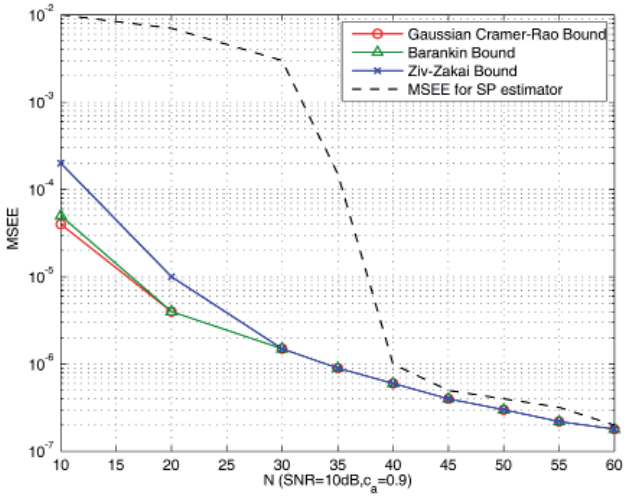

Figure 5. The mean-square estimation error as a function of N.

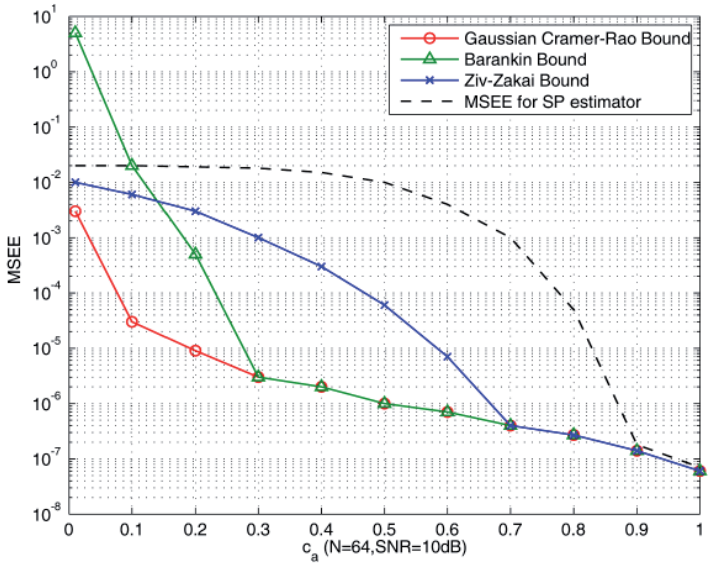

Figure 6. The mean-square estimation error as a function of c_a.

sufficiently large. The value of E_s/N_0 at which Cramer-Rao bound is close to the modified Cramer-Rao bound increases by about 6 dB when M doubles (PAM) or quadruples (QAM). This indicates that for uncoded pilot-symbol-free transmission, the convergence of the Cramer-Rao bound to the modified Cramer-Rao bound is mainly determined by the value of $\frac{E_s}{N_0}(d_M)^2$, with d_M denoting the minimum Euclidean distance between the constellation points. Furthermore, at the normal operating SNR of uncoded digital-communication systems, the Cramer-Rao bounds turn out to be very well approximated by the corresponding modified Cramer-Rao bounds.

7.2 Non-Constant Complex Amplitude = Gaussian

The multiplicative noise, $a(n)$, is hereafter assumed to be a white non-circular Gaussian process with zero mean, unit variance, and pseudo-variance $c_a = \mathbb{E}\left[a(n)^2\right]$. For the sake of simplicity, we also assume that the real part of $a(n)$ is independent of its imaginary part. This implies that c_a is real-valued. If $c_a = 0$, then $a(n)$ is circular; if $c_a = 1$, then $a(n)$ is real-valued. Thus, c_a quantifies the non-circularity rate of $a(n)$. We also set $\text{SNR [dB]} = 10\log_{10}\left(1/\sigma_w^2\right)$.

In each figure, we display four curves. Dashed lines correspond to the empirical mean-square estimation error for the well-known square-power (SP) estimate [1, 31, 34]. Solid lines with star-shape markers represent the Ziv-Zakai bound. Solid lines with triangular-shaped markers represent the Barankin bound. Solid lines with circular-shaped markers represent the Cramer-Rao bound [31, 53].

In Figure 4, we plot all the curves as a function of the SNR with $N = 64$, $c_a = 1$. We observed that the well-known outliers effect occurred at low and medium SNR [33]. We also observed that the Ziv-Zakai bound is significantly tighter than the Barankin bound. The SNR threshold corresponding to the SP-based estimate was much larger than that observed with the Barankin bound, while the threshold value predicted by the Ziv-Zakai bound was quite close to that obtained empirically with the square-power estimate. As a consequence, the Ziv-Zakai bound seems to be more powerful than the Barankin bound.

In Figure 5, we plot the curves as a function of N with $\text{SNR} = 10$ dB, $c_a = 0.9$. Even though the Ziv-Zakai bound offered a more realistic value for the N threshold than the Barankin bound, the mismatch between the Ziv-Zakai bound and the square-power mean-square estimation error performance was still quite large.

In Figure 6, the curves are displayed as a function of c_a with $N = 64$, $\text{SNR} = 10$ dB. One could notice that the more $a(n)$ was non-circular (i.e., c_a increased), the better the estimation performance. Furthermore, the outliers effect rapidly degraded the performance if $a(n)$ was not sufficiently non-circular. The figure confirmed that accurate frequency estimation is really difficult to achieve when the white signal is not sufficiently non-circular.

8. Conclusions

In this tutorial, we have focused on the derivation and the analysis of fundamental lower bounds on the achievable mean-square estimation error for estimating the frequency and the phase of a received signal, when the complex amplitude of the signal is non-constant and unknown. In particular, the following application fields have been considered: digital communications, direction-of-arrival estimation, and Doppler radar. An overview of lower bounds (the Cramer-Rao bound, modified Cramer-Rao bound, Barankin bound, and Ziv-Zakai bound), with their respective interests and their associated derivations in closed form for various cases, has been presented.

9. References

1. O. Besson and P. Stoica, "Nonlinear Least-Squares Approach to Frequency Estimation and Detection for Sinusoidal Signals with Arbitrary Envelope," *Digital Signal Processing*, **9**, 1, January, 1999, pp. 45-56.

2. M. Ghogho, A. K. Nandi, and A. Swami, "Cramer-Rao Bounds and Maximum Likelihood Estimation for Random Amplitude Phase-Modulated Signals," *IEEE Transactions on Signal Processing*, **47**, 11, November, 1999, pp. 2905-2916.

3. M. Ghogho, A. Swami, and T. S. Durrani, "Frequency Estimation in the Presence of Doppler Spread: Performance Analysis," *IEEE Transactions on Signal Processing*, **49**, 4, April, 2001, pp. 777-789.

4. H. Meyr, M. Moeneclaey and S. A. Fechtel, *Digital Communication Receivers, Volume 2, Synchronization, Channel Estimation, and Signal Processing*, New York, John Wiley & Sons, 1997.

5. C. Berrou, A. Glavieux and P. Thitimajsima, "Near Shannon Limit Error-Correcting Coding and Decoding: Turbo Codes," IEEE International Conference on Communications (ICC), May, 1993, Geneva, Switzerland, pp. 1064-1070.

6. R. G. Gallager. "Low Density Parity-Check Codes," *IRE Transactions on Information Theory*, **8**, 1, January, 1962, pp. 21-29.

7. D. J. C. MacKay. "Good Error-Correcting Codes Based on Very Sparse Matrices," *IEEE Transactions on Information Theory*, **45**, 2, March, 1999, pp. 399-431.

8. G. Caire, G. Taricco and E. Biglieri. "Bit-Interleaved Coded Modulation," *IEEE Transactions on Information Theory*, **44**, 3, May 1998, pp. 927-946.

9. N. A. D'Andrea, U. Mengali and R. Reggiannini, "The Modified Cramer- Rao Bound and its Application to Synchronization Problems," *IEEE Transactions on Communications*, **42**, 2/3/4, March 1994, pp. 1391-1399.

10. F. Gini, R. Reggiannini and U. Mengali. "The Modified Cramer-Rao Bound in Vector Parameter Estimation," *IEEE Transactions on Communications*, **46**, 1, January, 1998, pp. 52-60.

11. M. Moeneclaey, "On the True and the Modified Cramer-Rao Bounds for the Estimation of a Scalar Parameter in the Presence of Nuisance Parameters," IEEE Transactions on Communications, 46, 11, November, 1998, pp. 1536-1544.

12. W. G. Cowley, "Phase and Frequency Estimation for PSK Packets: Bounds and Algorithms," *IEEE Transactions on Communications*, **44**, 1, January, 1996, pp. 26-28.

13. F. Rice, B. Cowley, B. Moran and M. Rice. "Cramer-Rao Lower Bounds for QAM Phase and Frequency Estimation," *IEEE Transactions on Communications*, **49**, 9, September, 2001, pp. 1582-1591.

14. H. Steendam and M. Moeneclaey, "Low-SNR Limit of the Cramer-Rao Bound for Estimating the Carrier Phase and Frequency of a PAM, PSK or QAM Waveform," IEEE Communications Letters, 5, 5, May, 2001, pp. 215-217.

15. N. Noels, H. Steendam and M. Moeneclaey. "The True Cramer-Rao Bound for Carrier Frequency Estimation from a PSK Signal," *IEEE Transactions on Communications*, **52**, 5, May, 2004, pp. 834-844.

16. N. Noels, H. Steendam and M. Moeneclaey. "Carrier and Clock Recovery in (Turbo) Coded Systems: Cramer-Rao Bound and Synchronizer Performance," *EURASIP Journal on Applied Signal Processing*, **2005**, 6, May, 2005, pp. 972-980.

17. N. Noels, H. Steendam, M. Moeneclaey and H. Bruneel, "Carrier Phase and Frequency Estimation for Pilot-Symbol Assisted Transmission: Bounds and Algorithms," *IEEE Transactions on Signal Processing*, **53**, 12, December, 2005, pp. 4578-4587.

18. G. N. Tavares, L. M. Tavras and M. S. Piedade, "Improved Cramer- Rao Lower Bounds for Phase and Frequency Estimation with M-PSK Signals," *IEEE Transactions on Communications*, **49** ,12, December, 2001, pp. 2083-2087.

19. J. P. Delmas, "Closed-Form Expressions of the Exact Cramer-Rao Bound for Parameter Estimation of BPSK, MSK or QPSK waveforms," IEEE Signal Processing Letters, 15, April, 2008, pp. 504-508.

20. J. Ziv and M. Zakai. "Some Lower Bounds on Signal Parameter Estimation," *IEEE Transactions on Information Theory*, **15**, 3, May, 1969, pp. 386-391.

21. R. W. Miller and C. B. Chang. "A Modified Cramer-Rao Bound and its Applications," IEEE Transactions on Information Theory, 24, 3, May, 1978, pp. 398- 400.

22. F. Gini and R. Reggiannini, "On the Use of Cramer-Rao-Like Bounds in the Presence of Random Nuisance Parameters," IEEE Transactions on Communications, 48, 12, December, 2000, pp. 2120-2126.

23. J. Francos and B. Friedlander, "Bounds for Estimation of Multicomponent Signals with Random Amplitude and Deterministic Phase," IEEE Transactions on Signal Processing, 43, 5, May, 1995, pp. 1161-1172.

24. J. Francos and B. Friedlander, "Bounds for Estimation of Complex Exponentials in Unknown Colored Noise," IEEE Transactions on Signal Processing, 43, 9, September, 1995, pp. 2176-2185.

25. G. Zhou and G. B. Giannakis, "Harmonics in Gaussian Multiplicative and Additive White Noise: Cramer-Rao Bounds," *IEEE Transactions on Signal Processing*, **43**, 5, May, 1996, pp. 1217-1231.

26. G. Vazquez, *Signal Processing Advances for Wireless Mobile Communications*, Englewood Cliffs, NJ, Prentice-Hall, 2000, Chapter 9, "Non-Data-Aided Digital Synchronization."

27. E. W. Barankin, "Locally Best Unbiased Estimates," *Annals of Mathematical Statistics*, **20**, 1949, pp. 447-501.

28. H. Messer, "Source Localization Performance and the Array Beampattern," *Signal Processing Archive*, **28**, 2, August, 1992, pp. 163-181.

29. L. Knockaert, "The Barankin Bound and Threshold Behavior in Frequency Estimation," *IEEE Transactions on Signal Processing*, **45**, 9, September, 1997, pp. 2398-2401.

30. A. Renaux, P. Forster, P. Larzabal, C. Richmond, and A. Nehorai, "A Fresh Look at the Bayesian Bounds of the Weiss-Weinstein Family," IEEE Transactions on Signal Processing, 56, 11, November 2008, pp. 5334-5352.

31. P. Ciblat, M. Ghogho, P. Larzabal, and P. Forster, "Harmonic Retrieval in the Presence of Non-Circular Gaussian Multiplicative Noise: Performance Bounds," *Signal Processing Archive*, **85**, 4, April, 2005, pp. 737-749.

32. H. L. Van Trees, Detection, Estimation, and Modulation Theory, Part I, New York, John Wiley & Sons, 2001.

33. D. C. Rife and R. R. Boorstyn. "Single-Tone Parameter Estimation from Discrete-Time Observations," IEEE Transactions on Information Theory, 20, 9, September, 1974, pp. 591-598.

34. M. Ghogho, A. Swami, and A. K. Nandi, "Non Linear Least Squares Estimation for Harmonics in Multiplicative and Additive Noise," *Signal Processing Archive*, **78**, 1, October 1999, pp. 43-60.

35. A. Hansson, K. M. Chugg and T. M. Aulin, "On Forward-Adaptive versus Forward/Backward-Adaptive SISO Algorithms for Rayleigh Fading Channels," *IEEE Communications Letters*, **5**, 12, pp. 477-479.

36. N. Noels, *Synchronization in Digital Communication Systems: Performance Bounds and Practical Algorithms*, PhD dissertation, Faculty of Engineering, Ghent University, 2009, available at http://telin.ugent.be/\~nnoels.

37. N. Noels and M. Moeneclaey, "True Cramer-Rao Bound for Estimating Synchronization Parameters from a Linearly Modulated Bandpass Signal with Unknown Data Symbols," 2nd IEEE International Workshop on Computational Advances in Multi-Sensor Adaptive Processing (CAMSAP), Saint Thomas, VI USA, December, 2007.

38. H. A. Loeliger, "An Introduction to Factor Graphs," IEEE Signal Processing Magazine, 21, 1, January, 2004, pp. 28-41.

39. B. Picinbono, "On Circularity," *IEEE Transactions on Signal Processing*, **42**, 12, December, 1994, pp. 3473-3482.

40. B. Porat, Digital Signal Processing of Random Signals, Englewood Cliffs, NJ, Prentice Hall, 1994.

41. P. Whittle, "The Analysis of Multiple Stationary Time-Series," *Journal of Royal Statistics Society*, **15**, 1, January, 1953, pp. 125-139.

42. W. Jakes, Microwave Mobile Communications, New York, John Wiley & Sons, 1975.

43. R. Clarke, "A statistical Theory of Mobile Radio Reception," *Bell Systems Technical Journal*, **47**, June, 1968, pp. 957-1000.

44. R. M. Gray, "Toeplitz and Circulant Matrices: a Review," Stanford EE Lab. Report, 2002.

45. U. Grenander and G. Szegö, *Toeplitz Forms and their Applications*, Berkeley, University of California (Berkeley) Press, 1958.

46. E. J. Hannan, "The Estimation of Frequency," *Journal of Applied Probability*, **10**, 3, September, 1973, pp. 510-519

47. A. J. Viterbi and A. M. Viterbi, "Non-Linear Estimation of PSK-Modulated Carrier Phase with Application to Burst Digital Transmissions," *IEEE Transactions on Information Theory*, **29**, 7, July, 1983, pp. 543-551.

48. Y. Wang, E. Serpedin and P. Ciblat, "Optimal Blind Nonlinear Least Squares Carrier Phase and Frequency Offset Estimation for General QAM Modulations," *IEEE Transactions on Wireless Communications*, **2**, 9, September, 2003, pp. 1040-1054.

49. S. K. Chow and P. M. Schultheiss, "Delay Estimation Using Narrow-Band Processes," *IEEE Transactions on Acoustics, Speech, and Signal Processing*, **29**, 6, June, 1981, pp. 478-484.

50. K. L. Bell, Y. Steinberg, Y. Ephraim, and H. L. Van Trees, "Extended Ziv-Zakai Lower Bound for Vector Parameter Estimation," *IEEE Transactions on Information Theory*, **43**, 3, March, 1997, pp. 624-637.

51. Q. Zhang and D. Liu, "A Simple Capacity Formula for Correlated Diversity Rician Fading Channels," *IEEE Communications Letters*, **6**, 11, November 2002, pp. 481-483.

52. M. K. Simon and M. S. Alouini, "On the Distribution of Two Chi-Square Variates with Application to Outage Probability Computation," *IEEE Transactions on Communications*, **49**, 11, November, 2001, pp. 1946-1954.

53. P. Ciblat and M. Ghogho, "Ziv-Zakai Bound for Harmonic Retrieval in Multiplicative and Additive Gaussian Noise," IEEE Statistical Signal Processing Workshop (SSP), Bordeaux, France, July, 2005.

The Role of Radio Science in Disaster Management

P.J. Wilkinson
D.G. Cole

Abstract

Recent major natural disasters have brought a greater awareness of the social and economic deprivations that follow global emergencies. Among other organizations, URSI (International Union of Radio Science) is assessing its contribution, past and future, to the mitigation of natural and human-induced hazards.

This paper summarizes the way in which radio science has contributed to lessening the impact of disasters, both in the past and future. Its objective is to encourage all radio scientists to think how they can contribute further to alleviate the impact of disasters.

1. Introduction to URSI Inter-Commission WG1

Between 1975 and 2009, over 10,000 natural disasters worldwide killed more than 2,500,000 people, and produced estimated damages of over 1.7 trillion US dollars. Earthquakes, landslides, tropical cyclones, severe storms, floods, and infectious diseases were the major causes [1].

Science and technology working with society can reduce the risk and impact of disasters.

Radio science pervades society, and has an integral role in disaster management and mitigation that is often taken for granted. Radio is a vital element in monitoring the environment, and in feeding data to prediction models that are a major factor in safety and economic wellbeing [2]. When the telecommunication infrastructure is significantly or completely destroyed in a disaster, then radio communications (especially radio-amateur and satellite services) become important for disaster-relief operation. Building on radio research – which the URSI Commissions embrace – the International Telecommunication Union (ITU) and World Meteorology Organization (WMO) have developed recommendations, reports, and handbooks related to the use of radio communications to reduce the impact of natural and manmade disasters (including the anticipated effects of climate change) [3, 4].

In response to an increasing vulnerability to global disasters, the 2008 URSI General Assembly created a Working Group on Natural and Human Induced Hazards (WG1) [5], with the following terms of reference:

a) To study, within the URSI area of competence, methods and strategies related to natural and human-induced environmental hazards and disasters, such as:

   (i) Communication systems suitable for fast-response disaster relief;

   (ii) The development and application of remote-sensing products and other global data for monitoring and alerting;

   (iii) The evaluation of long-term and short-term risks of disasters, and;

   (iv) The description of the environment disturbances resulting from disasters;

b) To provide support to initiatives taken in the area of risk management and relief related to natural and human-induced catastrophes and disasters, particularly by developing countries.

This paper provides some background and ideas on ways in which URSI has contributed, and will continue to contribute, to the reduction of public risk from natural and human-induced hazards. The ideas and techniques presented here will be further refined. Readers are encouraged to contact the WG1 Chair and lead author (Phil Wilkinson) with any comments, ideas, and additional references, including Web references. This information will be added to the Working Group Web site, shortly to be linked to the URSI Web site (http://www.ursi.com).

2. Stages in Hazard Risk Reduction

It is practically impossible to prevent the occurrence of natural disasters and subsequent damage. However, it is possible to reduce the impact of disasters by the following:

P. J. Wilkinson and D. G. Cole are with IPS, Bureau of Meteorology, Australia; E-mail: phil@ips.gov.au.